

## DYNAMIC AND CYCLIC STATIC LOADING BEHAVIOR OF SILTY-SANDY CLAY AT SMALL AND MODERATE STRAINS

Katarzyna Gabryś, Wojciech Sas, Emil Soból

Warsaw University of Life Sciences – SGGW

**Abstract.** The shear modulus ( $G$ ) is one of the key parameters for seismic ground response analysis and it can be usually determined by means of dynamic tests ( $DT$ ), such as resonant column test ( $RCT$ ), or cyclic static test ( $CST$ ), e.g. torsional shear ( $TST$ ). The  $RC$  and  $TS$  tests are widely used laboratory methods to find stiffness of soil at small to medium strain range (0.0001–0.5%). The purpose of this paper is to present the experimental results from  $RC$  and  $CS$  laboratory tests on silty-sandy clay from the western part of Warsaw, Poland. The study aims to compare the shear modulus values obtained from two different research techniques. The influence of, in particular, the applied effective pressure, associated shear strain and experimental method (i.e. loading frequency and output amplitude) on the shear modulus at small strains ( $G_{\max}$ ) and secant shear modulus ( $G$ ) are investigated and proved. Generally, the results reveal that the examined soils stiffness calculated from  $TS$  tests is lower than from  $RC$  tests.

**Key words:** resonant column, torsional shear, clay, laboratory tests, stiffness

### INTRODUCTION

Soil stiffness at small strains is considered to be one of the most important parameter in solving boundary value problems, such as e.g.: dynamic interaction between soil and foundation, seismic reaction of soil deposits to earthquakes or special foundations' design for which only very small displacements are allowed to occur due to the serviceability limits [Lo Presti et al. 1993]. Many geotechnical engineers, among them were [Hardin 1978, Jardine 1985, Burland 1989], over the years, have postulated that  $G_0$  ( $\sim G_{\max}$ ) at small strains, smaller than the elastic threshold strain, appears as independent from the strain level as well as the shear stress level. An elastic or apparently elastic soil response

---

Corresponding author: Katarzyna Gabryś, Warsaw University of Life Sciences – SGGW, Faculty of Civil and Environmental Engineering, Water Centre – Laboratory, 6 Ciszewskiego St., 02-776 Warsaw, e-mail: katarzyna\_gabrys@sggw.pl

© Copyright by Wydawnictwo SGGW, Warszawa 2016

appears only at small strains, i.e. less than 0.001%. In reality, soil behavior is non linear (non linear elasticity or plasticity) and anisotropic, in the strain range from 0.001 to 1.0% [Lo Presti 1995]. Thus, an accurate evaluation of soil stiffness in the above range is of extreme significance.

Small-strain soil stiffness can be measured in laboratory and/or field tests [Benz 2007]. In laboratory, the shear modulus ( $G$ ) and damping ratio ( $D$ ) of soils are usually determined by means of cyclic static tests (e.g. torsional tests) or dynamic tests (i.e. resonant column tests) [Lo Presti et al. 1997]. Dynamic tests operate at higher frequencies than static, or quasi-static tests, in which effects caused by the inertia forces are considered negligible [Benz 2007]. Further differences between these types of tests are the loading rate ( $\dot{\gamma}$ ) and number of loading cycles ( $N$ ) [Lo Presti et al. 1997]. Characteristic of the static tests is that the cyclic loading stage is applied stepwise under strain or stress control, after the consolidation process is finished. Moreover, a certain number of loading cycles (e.g.  $N = 10, 100$ ) is placed to the specimen using sinusoidal or triangular variation of torque at constant frequency, mostly from the scope of 0.1–1.0 Hz. In the case of the resonant column tests it is not possible to control both  $\dot{\gamma}$  or  $N$ . The resonance frequency ( $f_n$ ) usually falls into the range of about 30–200 Hz, and, furthermore,  $N$  is as a rule of the order of thousands. Summarizing, the resonant column tests adopt much higher strain rates and impose a greater number of loading cycles on the soil specimen, in comparison to the static tests [Lo Presti et al. 1997].

In this paper, the results of resonant column test (*RCT*) and cyclic static test (*CST*), exactly from Torsional Shear (*TS*) Apparatus, performed on silty-sandy clay samples, of Quaternary origin, are presented. Both tests were carried out in the same device, though with some small modifications. The objective of the research was the following: comparing the results of the cyclic static torsional shear tests to those obtained under dynamic loading conditions, i.e. from *RCT*.

## EXPERIMENTAL TECHNIQUE AND TESTING PROCEDURES

The *RC* and *TS* apparatus used for the presented work is the Stokoe apparatus for a fixed-free configuration [Stokoe et al. 1980], manufactured in 2009 by the British company GDS Instruments Ltd, with its office in Hook, Hampshire, U.K. A detailed description of the apparatus can be found in [Gabryś et al. 2013, 2015, Sas et al. 2016]. Figure 1 shows a photograph of the resonant column device employed by the authors for the experiments discussed here. Laboratory test post with the GDS Resonant Column Apparatus is located in Water Centre-Laboratory, Warsaw University of Life Sciences – SGGW, Poland.

In the *RCTs*, the shear modulus ( $G$ ), corresponding to the particular shear strain, can be calculated from:

$$G = \rho \cdot V_S^2 \quad (1)$$

where:  $\rho$  is the specimen density and  $V_S$  is the shear-wave velocity. The shear-wave velocity ( $V_S$ ) can be found using:

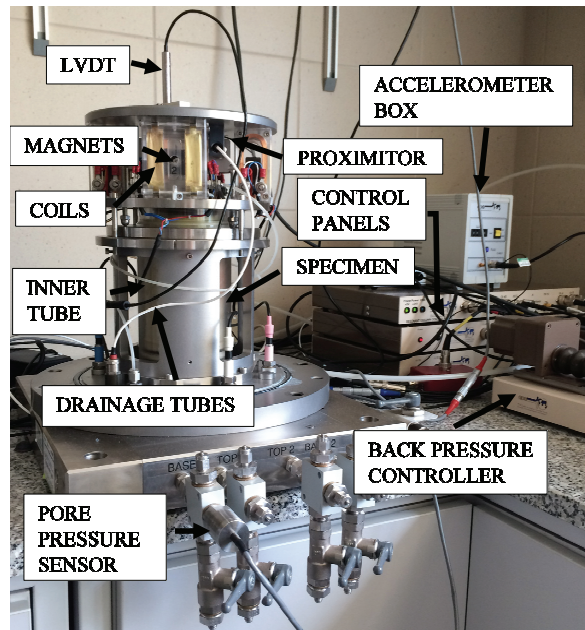


Fig. 1. Close-up view of the Resonant Column Apparatus

$$\frac{I}{I_0} = \frac{\omega \cdot h}{V_S} \tan\left(\frac{\omega \cdot h}{V_S}\right) \quad (2)$$

where:  $I$  is the mass polar moment of inertia of the specimen,  $I_0$  is the mass polar moment of inertia of the components mounted on the top of the specimen (drive system, top platen, etc.),  $\omega$  is the natural frequency of the first torsional mode of vibration,  $h$  is the height of the specimen [Fedrizzi et al. 2015].

The shear strain amplitude ( $\gamma$ ) can be compute with:

$$\gamma = \frac{r \cdot \theta}{h} \quad (3)$$

where:  $\theta$  and  $h$  are the twist angle and height of the section which the calculated point locates,  $r$  is the distance between the calculated point and the axis of the specimen. Usually, the top section of the specimen is used to evaluate the material properties. Hence,  $\gamma$  can be calculated from:

$$\gamma = \frac{r \cdot \theta_{\max}}{H} \quad (4)$$

in which

$$\theta_{\max} = \frac{x}{R} = \frac{x_A}{l_A} \quad (5)$$

The explanation of the other symbols is following:  $x$  = length of the arc which a given point at the edge of specimen during vibration,  $R$  = radius of examined cylindrical soil specimen,  $x_A$  = displacement of accelerometer mounted on the drive plate,  $l_A$  = offset of accelerometer from the axis of the specimen [Bai 2011].

During *CSTs*, a sinusoidal type of cyclic torsional load is applied at the top of specimen through a motor [Subramaniam and Banerjee 2016]. Soil specimen is vibrated with a low constant frequency (0.1–10Hz), for a finite number of cycles. Hysteresis loops are plotted and modulus  $G$  is obtained from:

$$G = \frac{\tau_{pp}}{\gamma_{pp}} \quad (6)$$

where:  $\tau_{pp}$  and  $\gamma_{pp}$  are the double-amplitude shear stress and strain respectively [Fedrizzi et al. 2015]. In Figure 2, the typical cyclic hysteretic loops in the shear stress – shear strain plane for clayey soils are presented. The loops were obtained from *TSTs* conducted at three different values of loading frequency ( $f = 0.1, 1.0$  and  $10$  Hz).

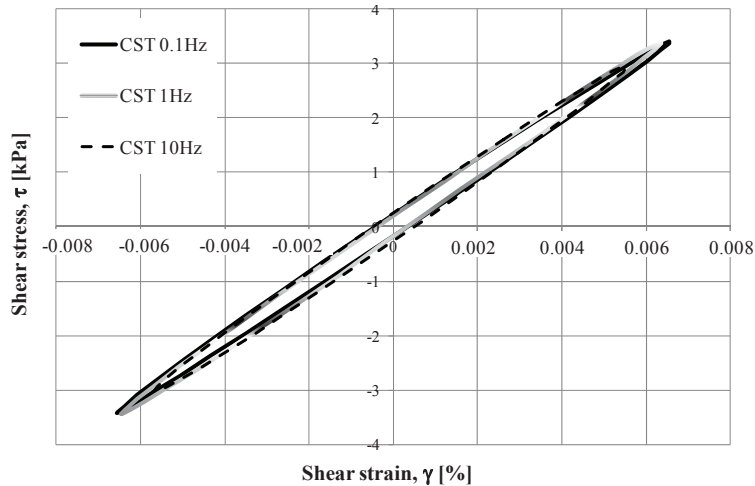


Fig. 2. Exemplary hysteresis loops for the output voltage 0.5V and mean effective stress 60 kPa

The *RC* torsional angle is measured generally by an accelerometer integrated with the excitation device or, e.g., by two displacement transducers (proximitor sensors) assembled at the top of the specimen. In *CST*, the angle of twist of the specimen is measured only through a proximitor sensor which faces the metal target.

In this study, it was possible to conduct both tests, *RCT* and *CST*, on the same soil specimen, without changing the apparatus settings. The comparison between the results received from these two above-described methods is infrequent, but is acceptable for a specific shear strain level. In this level, strain is verified to remain under elastic-plastic threshold by monitoring pre-straining effect as well as the cyclic degradation index.

*RC* studies and *CSTs* were performed on silty-sandy clay samples with a diameter of around 70 mm and a height of about 140 mm. After saturation process (Skempton's parameter *B* greater than 0.9), several stages of isotropic consolidation were carried out, for the particular consolidation pressure (30, 60, 90, 120, 150, 180, 210, 270, 330 and 370 kPa). First, resonant column (*RC*) experiments had been performed, around 24 hours after the consolidation stresses were applied. Then, the same specimens were subjected to cyclic loading. In *RCTs*, the number of applied loading cycles was of the order of thousands, while in *CSTs* was exactly 10. The output amplitude, which determines the amount of shear strain that is applied to the specimen, was from the range of 0.002 to 0.3 V for *RCT* and from the average range of 0.01 to 1.0 V for *CST*.

## PROPERTIES OF TESTING SOIL

The studied soil specimens included cohesive soil. In accordance with PN-EN 14688-1:2005 the laboratory tests were conducted on silty-sandy clay. High quality specimens were extracted from the depth approximately of 1.5 m with a thin-walled aluminum tube sampler. In Table 1, the main characteristics of the tested clayey soil are summarized. In Figure 3, grain-size distribution curve is given.

Table 1. Characteristics of the tested soil

Description	Unit	Value
Soil type acc. to PN-EN ISO 14688-1:2005	sasiCl	silty-sandy clay
Density of solid particles	g.cm <sup>-3</sup>	2.67
Bulk density of soil	g.cm <sup>-3</sup>	2.02
Dry density of soils particles	g.cm <sup>-3</sup>	1.70
Moisture content	%	18.25
Void ratio	–	0.57
Plastic limit	%	15.69
Liquid limit	%	32.60
Plasticity index	%	16.91
Liquidity index	–	0.08
Consistency index	–	0.081

The soil used in this work were obtained from the test site located in the western part of Warsaw, Poland. The exact location of the research area is around Pelczyńskiego Street, Bemowo district (Fig. 4). Warsaw is situated within the geological unit commonly known as Mazovian Basin or Warsaw Basin. This area was covered by Mindel and Riss Glaciations. Therefore, Bemowo district is characterized by a large number of anthropogenic soils, composed primarily of humus sands, gravels and bricks fragments. Below these anthropogenic soils, fine and medium sands, medium dense are located. Sandy soils are interbedded by cohesive – moraine clays, sandy clays and glacial lake deposits [Opracowanie ekofizjograficzne... 2006].

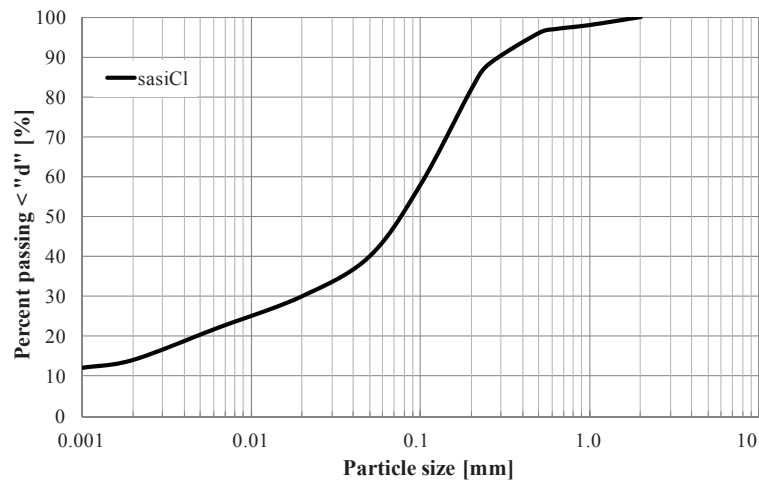


Fig. 3. Grain size distribution of the tested soil



Fig. 4. Study area as seen in Google Maps ([www.google.pl](http://www.google.pl))

## EXPERIMENTAL RESULTS AND DISCUSSION

Dynamic properties measured from both tests, *RCT* and *CST*, at shear strain amplitudes above and below a threshold limit, also referred to the shear modulus ( $G$ ) and the shear modulus at small-strains ( $G_{\max}$ ) respectively, are presented in this section. As the first results, the effect of the mean effective stress ( $p'$ ) on the hysteretic stress-strain loop of sandy-silty clay corresponding to the loading frequency  $f = 1.0$  Hz and the output amplitude  $A = 0.5$  V obtained by the *TSTs* are shown (Fig. 5). In the case of undisturbed clays, the secant shear modulus increases with an increase in confining pressure

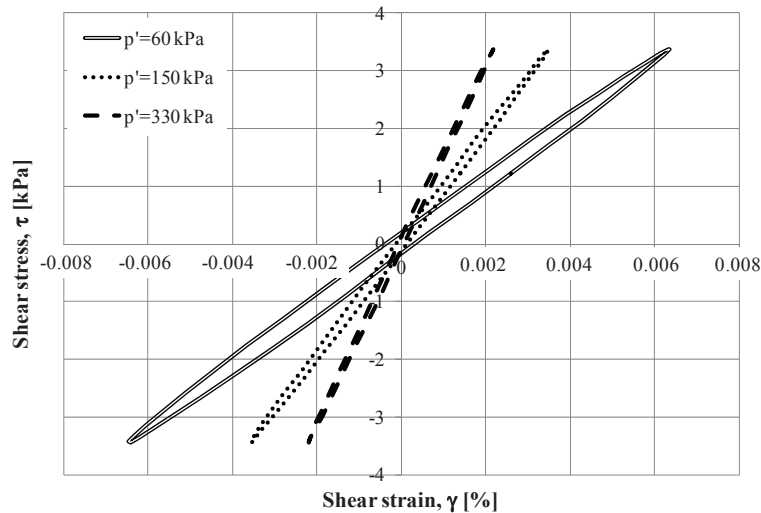


Fig. 5. Effect of mean effective stress in the hysteretic stress-strain loop from *TST*

[Ishibashi 1992], which is also reflected in this study. Similarly, the stress-strain loop rotates in the clock-wise direction with the increase in  $p'$ . As illustrated in Figure 5, the shear modulus values were received as follows:  $G = 53$  MPa for  $p' = 60$  kPa,  $G = 97$  MPa for  $p' = 150$  kPa and  $G = 155$  MPa for  $p' = 330$  kPa.

In Figure 6, the variation of  $G_{\max}$  with the mean effective stress for all tested specimens, along with the best-fit regression curves is presented. As expected, the applied isotropic stress has a significant influence on the  $G_{\max}$  values. For *RCT*, the increase in the  $G_{\max}$  values is from around 50 MPa to 173 MPa, respectively at the stress increase from 30 kPa to 370 kPa. For *CST*  $f = 0.1$  Hz,  $G_{\max}$  varies in the range of 41–206 MPa, for *CST*  $f = 1.0$  Hz  $G_{\max}$  is from the range of 44–212 MPa, whereas for *CST*  $f = 10$  Hz  $G_{\max} = 45$ –221 MPa. In the most presented cases, for similar  $p'$  the shear modulus at small strains from dynamic loading is greater than this obtained from cyclic static loading. The average difference between the  $G_{\max}$  values from the two kinds of loading is equal to 5 MPa (5%). For one value of  $p'$ , namely 370 kPa, higher  $G_{\max}$  value was obtained from *CST* than from *RCT*. This increase amounts to approximately 48 MPa (22%). It may be related to the relatively high pressure applied to specimen. In order to investigate carefully this effect, the authors suggest to use some other laboratory method, e.g. bender elements technique. In the case of this study, the soil type, as well as the hardware constraints, did not allow to continue further tests, at higher  $p'$  than 370 kPa. Therefore, it is not obvious how tested clay will behave.

The relationship between the shear modulus at small strains and the mean effective stress could be well fitted by power-law function  $f(x) = a \cdot x^{-k}$  (Fig. 6) calculated using the least squares approach. The coefficient of determination ( $R^2$ ) reaches the value greater than 0.94 in all types of conducted tests. Therefore, the proposed regression lines approximate very good the real points. The exponent ( $k$ ) values are very consistent, ranges from 0.4924 to 0.5586. It is similar with regard to the constant ( $a$ ) values. This variable amounts to from 6.0893 to 6.4799. This may indicate the same impact of  $p'$  on the  $G_{\max}$

values, regardless of the loading conditions. The authors stress, however, that their equations (Fig. 6) were developed for the specific clayey soil, i.e. Quaternary moraine clay, and can be applied only to the stress range from 30 to 370 kPa. For the stress' values greater than 370 kPa, other empirical formulas should be searched.

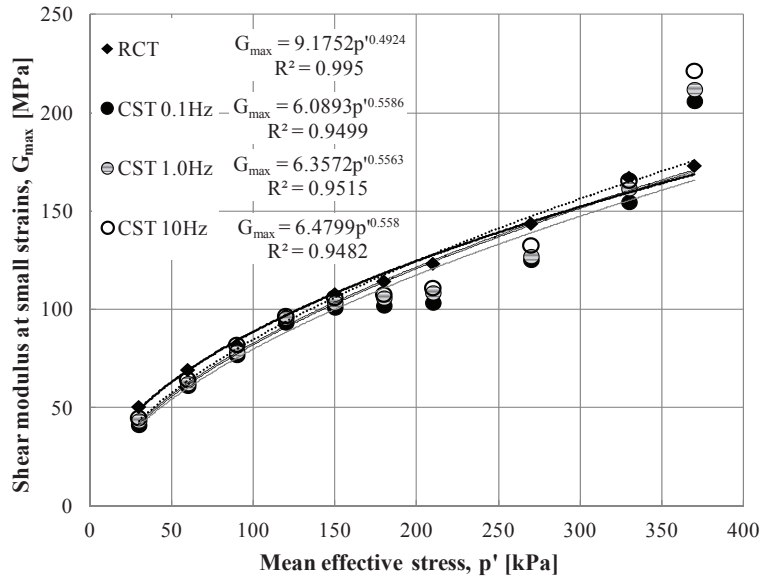


Fig. 6. Comparison of  $G_{\max}$  between *RCT* and *CST* results, performed consecutively on the same samples

In Figure 7, four shear modulus reduction curves obtained for the same mean effective stress  $p' = 30$  kPa are compared. This is another example of an influence of experimental procedure on the results. Analyzing Figure 7, it is possible to observe, that *RCTs* exhibit higher secant shear modulus values than *TSTs*. It may be noted as well, that in *CST* during low-frequency tests, i.e.  $f = 0.1$  Hz, the lowest  $G$  values were received. The highest frequency ( $f = 10$  Hz) used in *CST* allowed to get the highest  $G$  values among all those from *CSTs*. The difference between  $G_{RCT}$  and  $G_{CST10Hz}$  is about 5–10 MPa (11–24%).

In Figure 7, the degradation of the shear modulus with the shearing strain amplitude is presented as well. For the examined sandy-silty clay, the earlier observations of the authors, that is the increase in strain causes the decrease in the  $G$  values [Gabryś et al. 2015], from both dynamic and static tests, are confirmed. Similarly, considerable effect of confining pressure is observed in the normalized shear modulus curve, which is calculated from both tests. However, the effect of loading frequency and confining pressure diminish with an increase in the shear strain amplitude. It can be seen that the curves are increasingly closer to each one.

The variation in the normalized shear modulus ( $G/G_{\max}$ ) with the shear strain ( $\gamma$ ) for the tested materials is shown in Figure 8. In this figure, the  $G/G_{\max}$  values for all applied pressures in the authors' research are plotted in the form of a polynomial regression lines.

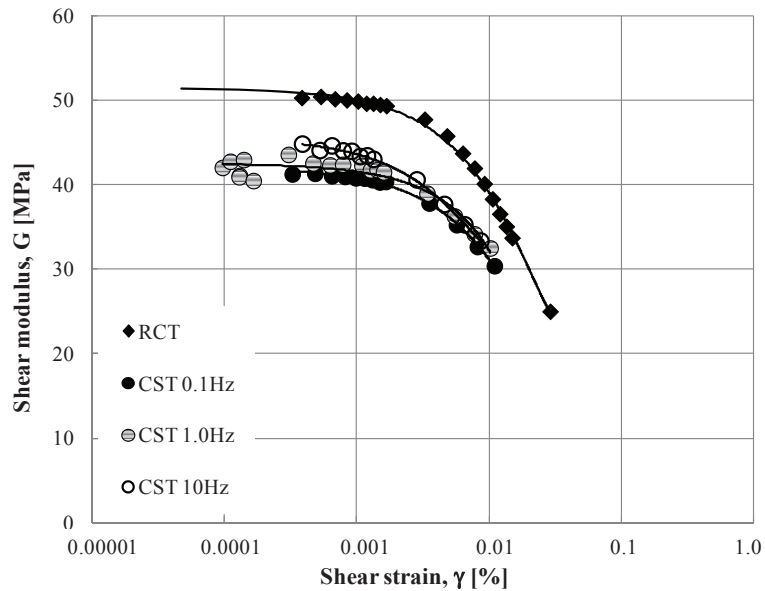


Fig. 7. Typical comparison of  $G$  from  $RC$  and  $CS$  tests at  $p' = 30$  kPa

From Figure 8, an apparent threshold shear strain value  $\gamma_{th} = 0.001\%$  can be readily established for all tested specimens, regardless of experimental procedure. The general trend is that the values of the normalized shear modulus with increasing shear strain amplitude tend to fall in relatively narrow band in both tests,  $RCT$  and  $CST$ .

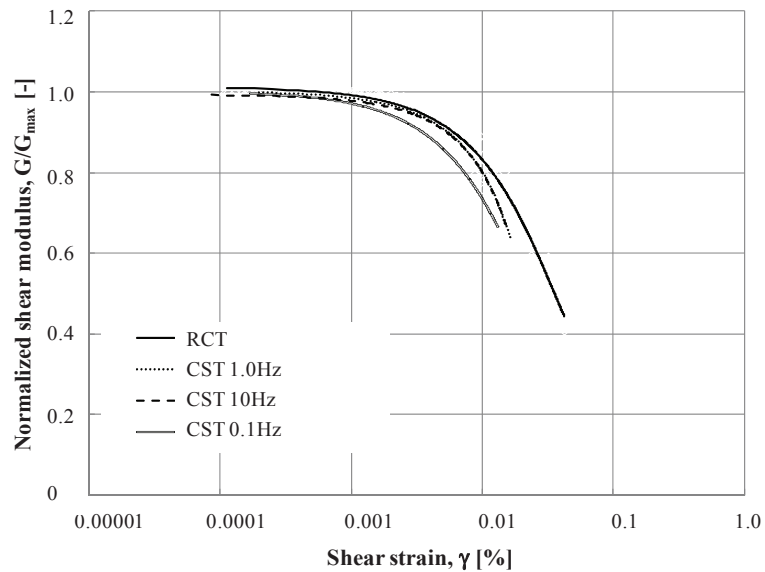


Fig. 8. Comparison of shear modulus reduction computed from  $RC$  and  $CS$  tests

To investigate the role of the output amplitude ( $A$ ) on the experiments, the shear modulus values were measured at different output amplitudes. The comparison of the received results for sandy-silty clay specimens at one selected stress (i.e.  $p' = 180$  kPa) is introduced in Figure 9. As already mentioned, the output amplitude informs about the voltage applied to the drive system. The *GDS RCA* software allows the user to put the maximum voltage of 1.0 V, to reduce any damage to the examined material. In order to ensure that the tested specimen is not overstrained, it is common to perform *RC* and *CS* tests in steps. This can be achieved by initially applying a very small voltage (e.g. 0.002 V) and then gradually increasing it. In Figure 9 can be noticed, that the lowest voltage placed (0.002 V when *RCT*) effects in the highest soil stiffness ( $G_{\max} \sim 114$  MPa). Up to a value  $A = 0.06$  V, the results from *RCTs* are greater than those from *TSTs*, with the maximum difference of around 7.6 MPa for the smallest output amplitude. The increase in the voltage applied to the system (namely  $> 0.06$  V) causes the reverse situation, the *CST* results are higher than *RCT* ones, from around 1 MPa ( $A = 0.07$  V) to 23 MPa ( $A = 0.3$  V). In the case of *RCTs*, a quite rapid drop in the  $G_{\max}$  values is observed, whereas for *CSTs* there is a mild decrease in  $G_{\max}$ . Above the amplitude 0.3V, the dynamic loading tests were stopped due to some problems in observation well-defined resonant frequency. This could also explain the higher  $G_{\max}$  values from *CST* than from *RCT*. Similar behaviour of tested clays for the output amplitude's changes was noticed at all mean effective stresses, but with a slightly different amplitude value limit, e.g. 0.04 V for  $p' = 30$  kPa.

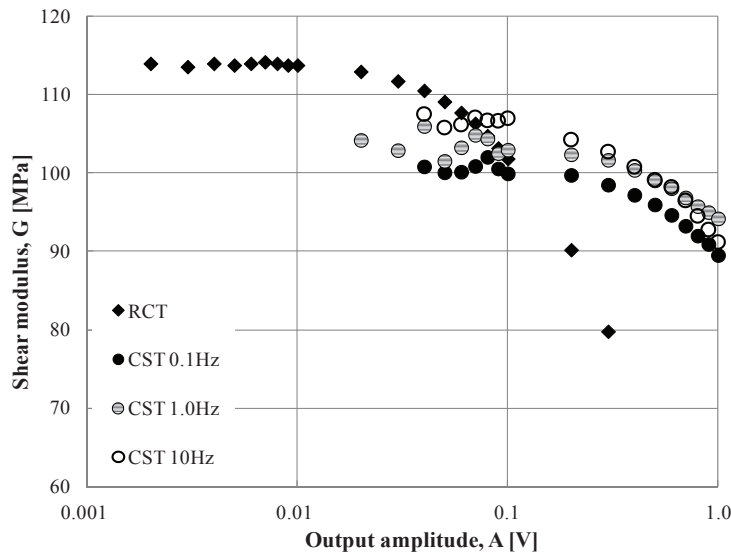


Fig. 9. Shear modulus v. output amplitude from *RC* and *CS* tests

*RC* tests were performed with the precise resonant frequency, while *CS* tests were repeated at different frequencies (0.1, 1.0 and 10 Hz) (see Fig. 10). The values of the shear modulus at small strains increase with frequency. The  $G_{\max}$  values from cyclic tests at  $f = 10$  Hz are the biggest ones, however the difference between  $G_{\max \text{ CST}10\text{Hz}}$  and  $G_{\max \text{ CST}0.1\text{Hz}}$  is in the range from 3.5 to 15.3 MPa, which is very low, as only approx. average 6%.



important, but also the mean effective stress which values were determined, should be reconsidered.

4. The dependency of the shear modulus on the strain level, regardless of applied experimental procedure was observed. This relationship was illustrated very well with polynomial regression lines. An apparent threshold shear strain value  $\gamma_{th} = 0.001\%$  can be readily recognized for all tested specimens.

5. Undisturbed silty-sandy clay turned out to be less sensitive to the test frequency, in *CST*. For example, the  $G_{max}$  values from the *CS* tests with  $f = 10$  Hz were only around 6% greater than those obtained from *CS* tests with  $f = 0.1$  Hz.

6. On the other hand, the presented results proved to be affected with the applied test method (*RCT* or *CST*).

7. In the next stage of their research, the authors would like to complement the laboratory tests with *in-situ* investigations. Thereby, the verification of the obtained results could be possible.

8. In research work, like presented article, it is important to develop regional relationships between studied parameters, e.g.  $G$  and others, for tested soils. Based on the results of *DTs* and *CSTs* on Quaternary moraine clays, as well as the review of the world literature, it can be ascertained that the dynamic and cyclic static loading behavior of this kind of soils is similar to soils formed in the other geological processes.

## REFERENCES

- Bai, L. (2011). Preloading Effects on Dynamic Sand Behavior by Resonant Column Tests. Ph. D. Thesis. Technical University of Berlin, Berlin.
- Benz, T. (2007). Small-Strain Stiffness of Soils and its Numerical Consequences. Ph.D. Thesis. University of Stuttgart, Stuttgart.
- Burland, J.B. (1989). Small is Beautiful-The Stiffness of Soil at Small Strains. Ninth Laurits Bjerrum Memorial Lecture. Canadian Geotechnical Journal, 26, 4, 499–516.
- Fedrizzi, F., Raviolo, P.L., Viganò, A., 2015. Resonant column and cyclic torsional shear experiments on soils of the Trentino valleys (NE Italy). Proc. 16<sup>th</sup> ECSMGE Geotechnical Engineering for Infrastructure and Development. ICE Publishing, 3437–3442.
- Gabryś, K., Sas, W., Szymański, A. (2013). Kolumna rezonansowa jako urządzenie do badań dynamicznych gruntów spoistych [In Polish]. Resonant Column Apparatus as a device for dynamic testing of cohesive soils. Przegląd Naukowy Inżynieria i Kształtowanie Środowiska. Scientific Review – Engineering and Environmental Sciences, 22 (1), 59, 3–13.
- Gabryś, K., Sas, W., Soból, E. (2015). Small-strain dynamic characterization of clayey soil. Acta Sci. Pol. Architectura, 14, 1, 55–65.
- Hardin, B.O. (1978). The Nature of Stress-Strain Behavior of Soils. Earthquake Engineering and Soil Dynamics. Pasadena CA, 1, 3–90.
- Ishibashi, I. (1992). Discussion of effect of soil plasticity on cyclic response by Mladem Vucetic and Ricardo Dobry. Journal of Geotechnical Engineering, 118, 5, 830–832.
- Jardine, R.J. (1985). Investigation of Pile-Soil Behavior with Special Reference to the Foundations off Offshore Structures. Ph.D. Thesis. University of London, London.
- Lo Presti, D.C.F. (1995). General report: Measurement of shear deformation of geomaterials in the laboratory. Proc. Int. Symp. on Pre-failure. Deformation of geomaterials. Ed. S. Shibuya, T. Mitachi and S. Muira, 2, 1067–1088.

- Lo Presti, D.C.F., Pallara, O., Lancellotta, R., Armandi, M., Maniscalco, R. (1993). Monotonic and Cyclic Loading Behavior of Two Sands at Small Strains. *Geotechnical Testing Journal*, 16, 4, 409–424.
- Lo Presti, D.C.F., Jamiolkowski, M., Pallara, O., Cavallaro, A., Pedroni, S. (1997). Shear modulus and damping of soils. *Géotechnique*, 47, 3, 603–617.
- Opracowanie ekofizjograficzne do studium uwarunkowań i kierunków zagospodarowania przestrzennego M. St. Warszawy. (2006). Urząd Miasta Stołecznego Warszawy, Warszawa.
- PN-EN 14688-1:2005. Geotechnical investigation and testing – Identification and classification of soil - Part 1: Identification and Description (ISO 14688-1:2002/Amd 1:2013).
- Sas, W., Soból, E., Gabryś, K., Markowska-Lech, K. (2016). Study of the cohesive soil stiffness in a modified resonant column. *Materiały Konferencji Naukowych. II Sympozjum Geofizyczne: APPLIED GEOPHYSICS 2016 – Geofizyka stosowana w zagadnieniach górniczych, inżynierskich i środowiskowych. 1–3 czerwca 2016, Gdańsk*, 1–15.
- Stokoe, K.H.II, Isehower, W.M., Hsu, J.R. (1980). Dynamic properties of offshore silty samples. *Proc. 12<sup>th</sup> Ann. Offshore Technology Conference*. Houston, Texas, 3771-MS.
- Subramaniam, P., Banerjee, S. (2016). Torsional Shear and Resonant Column Tests on Cement Treated Marine Clay. *Indian Geotechnical Journal*, 46, 2, 183–191.

## ZACHOWANIE SIĘ GLINY Z PYŁEM I PIASKIEM POD OBCIĄŻENIEM DYNAMICZNYM I CYKLICZNO-STATYCZNYM W ZAKRESIE MAŁYCH I ŚREDNICH ODKSZTAŁCEŃ

**Streszczenie.** Moduł odkształcenia postaciowego ( $G$ ) jest jednym z kluczowych parametrów w analizie odpowiedzi gruntu na oddziaływania sejsmiczne i zazwyczaj może być wyznaczony za pomocą badań dynamicznych, takich jak badania w kolumnie rezonansowej ( $RCT$ ), lub cykliczno-statycznych ( $CST$ ), na przykład skrętne ścinanie ( $TS$ ) bądź cykliczne badanie trójosiowe. Badania w kolumnie rezonansowej ( $RC$ ) oraz w aparacie skrętnego ścinania ( $TS$ ) są obecnie powszechnie stosowanymi metodami laboratoryjnymi pozwalającymi na znalezienie sztywności gruntu w zakresie małych i średnich odkształceń. Celem niniejszego artykułu jest przedstawienie wyników badań w kolumnie rezonansowej i w aparacie skrętnego ścinania wykonanych na glinie z pyłem i piaskiem, pochodzącej z zachodniej części Warszawy. Ponadto zamierzeniem autorów jest porównanie wartości modułów ścinania uzyskanych z dwóch różnych technik badawczych. Autorzy potwierdzają także istnienie wpływu w szczególności zastosowanego naprężenia efektywnego, poziomu odkształcenia oraz metody badawczej (tj. częstotliwości obciążenia i amplitudy napięcia na układzie napędowym) na moduł ścinania przy małych odkształceniach ( $G_{max}$ ) oraz na sieczny moduł ścinania ( $G$ ). Wyniki przeważnie pokazują, że sztywność badanego materiału obliczona na podstawie badań  $TS$  jest mniejsza niż ta uzyskana z badań  $RC$ .

**Słowa kluczowe:** kolumna rezonansowa, skrętne ścinanie, glina, badania laboratoryjne, sztywność

Accepted for print: 28.11.2016

For citation: Gabryś, K., Sas, W., Soból, E. (2016). Dynamic and cyclic static loading behavior of silty-sand clay at small and moderate strains. *Acta Sci. Pol. Architectura*, 15 (4), 43–55.